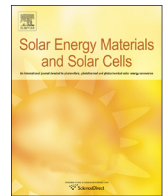




Contents lists available at SciVerse ScienceDirect

# Solar Energy Materials & Solar Cells

journal homepage: [www.elsevier.com/locate/solmat](http://www.elsevier.com/locate/solmat)

## Evaluation of implantation annealing for highly-doped selective boron emitters suitable for screen-printed contacts

Ralph Müller<sup>a,\*</sup>, Jan Benick<sup>a</sup>, Nicholas Bateman<sup>b</sup>, Jonas Schön<sup>a</sup>, Christian Reichel<sup>a</sup>, Armin Richter<sup>a</sup>, Martin Hermle<sup>a</sup>, Stefan W. Glunz<sup>a</sup>

<sup>a</sup> Fraunhofer Institute for Solar Energy Systems (ISE), Heidenhofstrasse 2, D-79110 Freiburg, Germany

<sup>b</sup> Applied Materials—Varian Semiconductor Equipment, 35 Dory Road, Gloucester, MA 01939, USA

### ARTICLE INFO

#### Keywords:

Silicon solar cells  
Ion implantation  
*n*-Type  
Selective emitter  
Annealing

### ABSTRACT

Ion implantation is a technology suitable for the formation of high quality junctions in silicon solar cell processing. As screen-printing is the state of the art metallization technique for industrial solar cells, the compatibility of ion implanted boron emitters with this metallization technique will be investigated. The fact that selective emitter structures can be *in situ* formed allows a high freedom in the design of the final emitter structure to meet the different demands of the metallized and passivated part of the emitter. In this work we investigate high dose implantations for the metallized area and low dose implantations for the passivated area that subsequently receive a short furnace anneal at 950 or 1050 °C. Applying a high dose in the range of  $3 \times 10^{15} \text{ cm}^{-2}$  high surface concentrations of around  $6 \times 10^{19} \text{ cm}^{-3}$  can be reached, allowing for a good contact of the screen-printed metallization. The passivated part of the emitter can be realized by implanting a lower dose ( $< 1 \times 10^{15} \text{ cm}^{-2}$ ). The sheet resistance is in the range of 110–160  $\Omega/\text{sq}$  resulting in very low emitter saturation current densities between 10 and 40  $\text{fA}/\text{cm}^2$ . Those experimental results demonstrate that ion implantation of selective boron emitters is compatible with industrial screen-printing technology and enables high cell efficiencies.

© 2013 Elsevier B.V. All rights reserved.

### 1. Introduction

Due to the development of high throughput ion implantation tools during the last years [1], this technology has sparked great interest as it offers several advantages compared to doping from a furnace diffusion. Especially for advanced solar cell concepts, the single side processing and the possibility to have a structured doping by *in situ* masking [2] without costly deposition, structuring as well as removal of masks, offer the path to cost effective manufacturing. Furthermore, ion implantation has the potential to increase the production efficiency of simple cell concepts due to the very high sheet resistance uniformity [3] and the fact that no edge isolation is necessary.

In a previous work we have shown  $J_{0e}$  of less than 10  $\text{fA}/\text{cm}^2$  for boron-implanted emitters with an alumina passivation [4]. Implemented into different high-efficiency cell concepts with passivated rear sides this implanted-boron emitter enabled an open-circuit voltage  $V_{OC}$  of more than 690 mV and a cell efficiency of 22.3%. This proves the feasibility to anneal the crystal damage introduced

by the boron implantation completely. The next step is to develop a process route for implanted boron emitters on *n*-type silicon solar cells enabling  $> 20\%$  efficiency at a low production cost. Therefore, it is to combine all the advantages of ion implantation together with a high quality surface passivation while being compatible with the screen-printing technology which is still the dominating metallization technique in production lines.

Several publications have been made showing cell efficiencies of around 19% on *n*-type silicon solar cells with ion-implanted boron emitters [5–7]. They all used a blanket emitter passivated by a thermal oxide grown during the furnace annealing covered by a silicon nitride as anti-reflection coating. The metallization has been realized by a screen-printing step. Ok et al. [8] reached a slightly higher efficiency of 19.6% with the same cell concept but an improved passivation of the boron emitter.

In this work we investigate different annealing conditions of boron implantations in order to find processes routes suitable to form a selective emitter. The surface concentration ( $N_{\text{Surf}}$ ) of boron in the metallized part of the emitter should be as high as possible to minimize the contact resistance to the printed metal. Recently it has been shown that contact resistances as low as 3  $\text{m}\Omega/\text{cm}^2$  can be achieved with an aerosol-printed ink on a boron emitter with  $N_{\text{Surf}}$  of  $2.3 \times 10^{19} \text{ cm}^{-3}$  [9], so we expect a good electrical contact of screen-printed pastes to implanted boron emitters with  $N_{\text{Surf}} > 3 \times 10^{19} \text{ cm}^{-3}$ .

\* Corresponding author. Tel.: +49 (0) 761/4588 5921;

fax: +49 (0) 761/4588 9250.

E-mail address: [ralph.mueller@ise.fraunhofer.de](mailto:ralph.mueller@ise.fraunhofer.de) (R. Müller).

Further, the profile underneath the metallization should be relatively deep to effectively shield the high surface recombination at the metal contact. The profile at the passivated part of the emitter should contain a significantly lower doping, but the sheet resistance has to remain at a certain level to provide a sufficient lateral conductivity and to keep the series resistance of the solar cell low. In order to enable high  $V_{OC}$  the saturation current density of the passivated emitter ( $J_{0e,pass}$ ) has to be as low as possible. This requires a low amount of doping, an effective annealing of the implantation damage and a good surface passivation. Typically, a screen-printed solar cell has a relatively high metal coverage which means that the overall emitter saturation current density ( $J_{0e}$ ) is significantly influenced by the saturation current density of the metallized part of the emitter ( $J_{0e,metal}$ ). Using the selective emitter approach, implantation conditions for the metallized and the passivated part can be optimized independently.

The goal of this work is to find process conditions for the implantation of selective boron emitters with

- Surface concentration of about  $5e19 \text{ cm}^{-3}$  for a good contact of the screen-printed paste to the metallized part of the emitter
- Sheet resistance  $< 150 \Omega/\text{sq}$  and emitter saturation current density  $< 50 \text{ fA}/\text{cm}^2$  in the passivated area to allow low series resistance and high  $V_{OC}$  at the device level.

## 2. Experimental

Symmetrical lifetime samples were prepared on  $10 \Omega \text{ cm}$   $n$ -type FZ silicon. They first received an RCA clean followed by a boron implantation (Varian VISta HC) on both sides with doses between  $5e14$  and  $1e16 \text{ cm}^{-2}$ . Then all samples received an SC2 clean before entering the tube furnace for annealing. For this process a non-oxidizing atmosphere and a short peak time (10 min) at temperatures of 950 and 1050 °C have been applied. After the anneal the samples were dipped in HF (1% HF) and received an alumina passivation (PE-ALD) followed by a forming gas anneal for 25 min at 425 °C to activate the passivation. QSSPC measurements were done with a WCT110 tester. For the highly-doped samples to be applied as the metallized emitter part the alumina was etched and a second QSSPC measurement was done. The sheet resistance was determined with a four point probe measurement tool and finally the profiles were measured by electrochemical capacitance-voltage (ECV) profiling. For some samples also a reference has been measured by secondary ion mass spectrometry (SIMS).

## 3. Results and discussion

### 3.1. Simulations

We used the commercial simulation tool Sentaurus Process [10] in order to determine a promising range of process conditions for implantation and annealing experiments. Starting from the high-efficiency emitter applied in an earlier work for the processing of high-efficiency solar cells [4], there are mainly two possible ways to increase the surface concentration which is necessary for a good electrical contact with a screen printed paste: (i) increasing the dose and (ii) decreasing the thermal budget of the anneal. The simulations in Fig. 1 illustrate this effect. There, the deeply driven-in high-efficiency emitter is plotted together with the simulated profile. The simulation models were calibrated to a wide range of implantation and annealing processes [11] and show a good match between measured and simulated data. For the high-efficiency emitter an oxidizing anneal was used [12]. This causes a fair amount of boron to be incorporated in the  $\text{SiO}_2$  and an

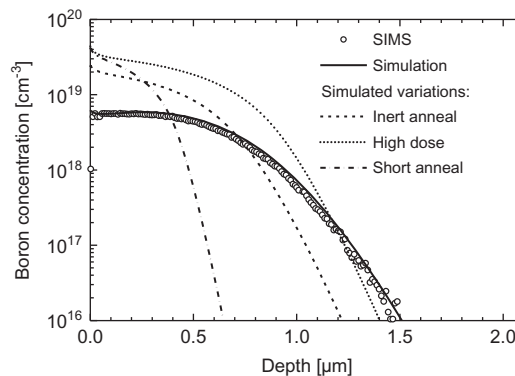


**Fig. 1.** SIMS profile of the implanted boron emitter used for high-efficiency silicon solar cells [4] and Sentaurus simulations of boron profiles after the same process conditions. Three further simulations show the effect of process variations: non-oxidizing anneal (inert anneal), double dose implantation+non-oxidizing anneal (high dose) and short non-oxidizing anneal (short anneal).

increased profile depth due to the enhanced diffusivity of boron in an oxidizing ambient [11]. According to this, the simulation of the same process but with an inert anneal shows a reduced depth and a significantly increased surface concentration (see Fig. 1). Two more simulations again with an inert anneal are shown in Fig. 1, (i) with twice the implanted dose and (ii) with a much shorter annealing. In both cases the surface concentration is further increased.

To allow for a fast processing it is favorable to keep the dose and the annealing duration as low as possible. The challenge is to have a short annealing enabling a sufficient thermal budget to electrically activate the implanted boron and to remove the implantation damage. Since the implantation of boron is non-amorphizing for doses below  $2e16 \text{ cm}^{-2}$  [13], the damage depends on the boron dose. Hence with increasing dose an increasing thermal budget is required for a sufficient damage anneal.

### 3.2. Experiments

From the simulations a promising range for experimental conditions was extracted. This is a “low dose” implantation range of  $5e14$ – $1e15 \text{ cm}^{-2}$  for the passivated part of the emitter and a “high dose” range of  $3e15$ – $1e16 \text{ cm}^{-2}$  for the metallized part of the emitter. A short furnace annealing with a peak time of 10 min was chosen at temperatures of 950 and 1050 °C. Fig. 2 shows the measured ECV profiles of all the samples processed under the aforementioned conditions. The junction depth strongly depends on the thermal budget. For the 950 °C anneal all profiles are very shallow, even for the high dose implantations. Increasing the temperature raises the depth up to more than  $1 \mu\text{m}$  for doses  $\geq 5e15 \text{ cm}^{-2}$  after the short 1050 °C anneal. In contrast, the surface concentration does not depend strongly on the temperature. The maximum doping concentration slightly increases with temperature from  $\sim 6e19 \text{ cm}^{-3}$  for 950 °C to  $\sim 8e19 \text{ cm}^{-3}$  for 1050 °C.

With the 950 °C anneal the highest surface concentration is already reached at implantation doses of  $3e15 \text{ cm}^{-2}$ . Hence the surface concentration is limited (given peak duration of 10 min) by the anneal temperature and cannot be increased by a higher implantation dose. This saturation effect causes the ECV profiles to coincide for implanted doses  $\geq 3e15 \text{ cm}^{-2}$  at 950 °C. At 1050 °C this saturation probably sets in at doses  $> 1e16 \text{ cm}^{-2}$ .

The saturation effect can be explained by the huge amount of boron near to the surface after the implantation. This seems to act as an inexhaustible doping source during the annealing if the thermal budget is not sufficient to drive all the boron into the substrate. The comparison of SIMS and ECV measurements shown in Fig. 3 supports this theory. In general the SIMS and ECV profiles

Download English Version:

<https://daneshyari.com/en/article/10248774>

Download Persian Version:

<https://daneshyari.com/article/10248774>

[Daneshyari.com](https://daneshyari.com)